Gravitational energy loss in high energy particle collisions: Ultrarelativistic plunge into a multidimensional black hole

Emanuele Berti*

Department of Physics, Aristotle University of Thessaloniki, Thessaloniki 54124, Greece
and McDonnell Center for the Space Sciences, Department of Physics, Washington University, St. Louis, Missouri 63130, USA

Marco Cavaglià†

Institute of Cosmology and Gravitation, University of Portsmouth, Portsmouth PO1 2EG, United Kingdom
and Department of Physics and Astronomy, The University of Mississippi, P.O. Box 1848, University, Mississippi 38677-1848, USA

Leonardo Gualtieri‡

Dipartimento di Fisica "G. Marconi," Università di Roma "La Sapienza," Italy
and Sezione INFN Roma 1, piazzale Aldo Moro 2, I-00185 Roma, Italy

We investigate the gravitational energy emission of an ultrarelativistic particle radially falling into a D-dimensional black hole. We numerically integrate the equations describing black hole gravitational perturbations and obtain the energy spectra, total energy, and angular distribution of the emitted gravitational radiation. The black hole quasinormal modes for scalar, vector, and tensor perturbations are computed in the WKB approximation. We discuss our results in the context of black hole production at the TeV scale.

I. INTRODUCTION

Brane-world models describe the visible Universe as a four-dimensional brane embedded in a higher-dimensional bulk [1]. A generic consequence of the brane-world scenario is that the fundamental gravitational scale is lower than the observed Planck scale. In some models, the fundamental scale is lowered to values that would be accessible to next-generation particle colliders, thus enabling laboratory-based studies of strong gravitational physics via perturbative [2] and nonperturbative events [3]. Ultrahigh energy cosmic rays could also probe trans-Planckian energies [4]. The possibility that strong gravitational effects such as black hole (BH) and brane formation could be observed in the near future has sparked a lot of interest in the investigation of nonperturbative gravitational phenomena in hard-scattering events [5]. (For a review and more references, see Ref. [6].)

Trans-Planckian BH formation at energy scales much larger than the fundamental gravitational scale is a classical process [3]. The event is dominated by the s channel and the initial state is modeled by two classical shock waves with given impact parameter. In this context, a major issue is the estimate of the collisional energy loss. The hoop conjecture states that the collision of two particles ij with center-of-mass (c.m.) energy $E_{\rm cm}$ and impact parameter smaller than the Schwarzschild radius $r_s(E_{\rm cm})$ forms a trapped surface [7]. This event is formally described by the process

$ij \rightarrow {\rm BH} + E(X)$, where $E(X)$ denotes the collisional "junk" energy which does not contribute to the BH mass. The junk energy includes a bulk component of gravitational radiation and other possible nonstandard model gauge fields, and a brane component of standard model collisional by-products carrying the charge of the initial particles. The newly formed BH is expected to decay first by loss of gauge radiation into the bulk and then by thermal Hawking emission. The Hawking evaporation ends when the mass of the BH approaches the fundamental gravitational scale. At this stage the BH either decays completely by emitting the residual Planckian energy or leaves a stable remnant with mass about the Planck mass [8]. Most of the observable signatures of BH formation come from Hawking's phase and strongly depend on the initial BH mass [9]. Hence, a precise calculation of the collisional energy loss is essential to the phenomenology of BH formation.

A numerical estimate of the total collisional energy loss for spherically symmetric BHs in $D \geq 4$ dimensions has been given by Yoshino and Nambu (YN) [10] (see also Ref. [11]). The YN approach evaluates the total junk energy $E(X)$ by investigating the formation of the BH apparent horizon [12]. The colliding particles are assumed massless, uncharged, and pointlike. Each particle is modeled by an infinitely boosted Schwarzschild solution with fixed energy. This solution describes a plane-fronted gravitational shock wave corresponding to the Lorentz-contracted longitudinal gravitational field (Aichelburg-Sexl wave) [13]. The collision is simulated by combining two shock waves traveling in opposite directions. The apparent horizon arises in the union of the two shock waves. The junk energy is estimated by comparing the initial c.m. energy with the BH mass. The result is that the collisional energy loss depends on the impact parameter and increases as the number of spacetime dimensions increases.

The YN method allows estimation of the total junk energy

---

*Present address: Groupe de Cosmologie et Gravitation (GReCO), Institut d'Astrophysique de Paris (CNRS), 98bis Boulevard Arago, 75014 Paris, France. Email address: berti@astro.auth.gr

†Email address: cavaglia@phy.olemiss.edu

‡Email address: leonardo.gualtieri@roma1.infn.it

in the classical uncharged point-particle approximation. However, it cannot discriminate between different components of $E(X)$, which is theoretically and experimentally most important. In a realistic BH event such as a proton-proton collision at the Large Hadron Collider (LHC) [14], the BH is formed by the collision of two partons. The bulk component of the junk energy is dominated by gravitational radiation and is invisible to the detector. The gravitational junk energy and the invisible component of Hawking emission (neutrinos, gravitons, etc.) add to the total missing energy of the process. Therefore, the knowledge of collisional energy loss in gravitational emission should provide a good estimate of the different sources of energy loss and missing energy.

An accurate estimate of the gravitational collisional energy loss would require the use of the full nonlinear Einstein equations in D dimensions. This is a formidable task, even in four dimensions. Recently, significant advances in numerical relativity allowed stable numerical simulations of BH-BH collisions for initial BH separation of a few Schwarzschild radii in the nonlinear Einstein theory. The gravitational waveforms predicted by these simulations are in excellent agreement with analytical results from first and second order perturbation theory [15]. Since the linearization of the Einstein equations yields results that are surprisingly close to the full theory (see, e.g., Ref. [16]), BH perturbation theory is likely to provide accurate estimates of gravitational wave emission in higher-dimensional spacetimes. Relying on this result, we compute the gravitational wave emission in higher dimensions via a perturbative approach. Our computation is the first of this kind to our knowledge.

The formalism for the computation of gravitational wave emission from perturbed BHs was developed by Regge and Wheeler [17] and Zerilli [18], who reduced the problem to the solution of two Schrödinger-like equations. Davis *et al.* [19] computed the energy radiated in the radial infall of a particle of mass m_0 starting from rest at infinity into a four-dimensional BH of mass $M_{BH} \gg m_0$. This study was later generalized to the radial infall of a particle with finite initial velocity or starting at a finite distance from the BH [20]. (For a more comprehensive introduction to BH perturbation theory see, e.g., Refs. [21].) Cardoso and Lemos [22,23] have recently investigated the plunge of ultrarelativistic test particles into a four-dimensional static BH and along the rotation axis of a Kerr BH, improving early estimates by Smarr [24]. In this paper we generalize these results to higher dimensions by computing the gravitational radiation emitted by an ultrarelativistic particle falling into a D-dimensional spherically symmetric BH. Since wave propagation in odd-dimensional curved spacetimes is not yet fully understood, we restrict our investigation to even dimensions. (Wave late-time behavior and propagation are very different in odd- and even-dimensional spacetimes [25–27]. Moreover, open issues in the definition of asymptotic flatness [28] do not allow an unambiguous definition of "gravitational waves radiated at infinity" in odd dimensions.)

We model the particle collision as a relativistic test particle plunging into a BH with mass $M_{BH} = E_{cm}$. We use recent results of D-dimensional gravitational-wave theory by

Cardoso *et al.* [25] and the D-dimensional extension of Zerilli's formalism by Kodama and Ishibashi (KI) [29–32], which reduces the problem to the solution of three Schrödinger-like equations. Our method provides a simple and relativistically consistent estimate of the collisional gravitational emission in higher dimensions. We derive the emitted energy in terms of the wave amplitude and study the angular dependence of the radiation using the KI formalism. We also present a systematic calculation of BH quasinormal modes (QNMs) for the different perturbations in the WKB approach, extending recent calculations by Konoplya [33,34]. We show that there is a significant relation between the QNM frequencies and the spectral content of the emitted radiation.

The outline of the paper is as follows. In Sec. II we introduce our notations and the basic equations. In Sec. III we briefly describe our numerical approach to the computation of gravitational wave emission (details are in the Appendixes). Section IV contains the main results of the paper. Conclusions are presented in Sec. V.

II. PERTURBATION EQUATIONS AND QUASINORMAL MODES

In the next subsection we introduce the background metric and the KI perturbation equations [30]. In Sec. II B we describe the method to compute the BH QNMs.

A. Background metric and perturbation equations

The spherically symmetric BH in $D = n+2$ dimensions is described by the Schwarzschild-Tangherlini metric [35]

$$ds^2 = -f(r)dt^2 + \frac{dr^2}{f(r)} + r^2 d\Omega_n^2, \tag{1}$$

where $d\Omega_n$ is the metric of the n-dimensional unit sphere S^n, and

$$f(r) = 1 - \frac{2M}{r^{n-1}}. \tag{2}$$

The BH mass M_{BH} is given in terms of the parameter M by

$$M_{BH} = \frac{nM\mathcal{A}_n}{8\pi c^2 G_{n+2}}, \tag{3}$$

where $\mathcal{A}_n = 2\pi^{(n+1)/2}/\Gamma((n+1)/2)$ is the area of S^n, G_{n+2} is the $(n+2)$-dimensional Newton constant, and c is the speed of light. We will set $G_{n+2} = 1$ and $c = 1$ in the following. The $(n+2)$-dimensional tortoise coordinate r_* is defined by

$$\frac{dr_*}{dr} = \frac{1}{f(r)}. \tag{4}$$

Integrating Eq. (4) we find

$$r_* = r + \frac{2M}{n-1} \sum_{j=0}^{n-2} \frac{\ln(r/\alpha_j - 1)}{\alpha_j^{n-2}}, \tag{5}$$

where

$$\alpha_j = (2M)^{1/(n-1)} e^{2\pi ij/(n-1)} \quad (j=0,\ldots,n-2), \quad (6)$$

and the integration constant has been chosen to make the argument of the logarithm dimensionless. Here and throughout the paper we use the notations of Refs. [29,30]; the indices (μ,ν), (i,j), and (a,b) denote the coordinates of the D-dimensional spacetime, the coordinates of S^n, and the coordinates of the two-dimensional spacetime (t,r), respectively.

Kodama and Ishibashi [30] showed that the gravitational perturbation equations for this metric can be reduced to Schrödinger-like wave equations:

$$\left(\frac{d^2}{dr_*^2} + \omega^2 - V \right) \Phi = 0, \quad (7)$$

where the potential V depends on the kind of perturbation. Setting $x \equiv 2M/r^{n-1}$, the potential for scalar perturbations is

$$V_S = \frac{f(r)Q(r)}{16r^2 H^2}, \quad (8)$$

where

$$\kappa^2 = l(l+n-1), \quad l=0, \ 1, \ 2, \ldots,$$

$$m = \kappa^2 - n, \quad H(r) = m + \frac{n(n+1)}{2}x, \quad (9)$$

and

$$Q(r) = n^4(n+1)^2 x^3 + n(n+1)[4(2n^2-3n+4)m$$
$$+ n(n-2)(n-4)(n+1)]x^2 - 12n[(n-4)m$$
$$+ n(n+1)(n-2)]mx + 16m^3 + 4n(n+2)m^2. \quad (10)$$

Equation (8) reduces to the Zerilli equation [18] for $n=2$. The potential for vector perturbations is

$$V_V = \frac{f}{r^2} \left[\kappa_V^2 + 1 + \frac{n(n-2)}{4} - \frac{3n^2 M}{2r^{n-1}} \right], \quad (11)$$

where

$$\kappa_V^2 = l(l+n-1) - 1, \quad l=1, \ 2, \ldots. \quad (12)$$

Equation (11) reduces to the Regge-Wheeler equation [17] for $n=2$. Finally, the potential for tensor perturbations is

$$V_T = \frac{f}{r^2} \left[\kappa_T^2 + 2 + \frac{n(n-2)}{4} + \frac{n^2 M}{2r^{n-1}} \right], \quad (13)$$

where

$$\kappa_T^2 = l(l+n-1) - 2, \quad l=1, \ 2, \ldots. \quad (14)$$

Equation (13) was derived by Gibbons and Hartnoll [36] in a more general case (see also Ref. [37], where a Gauss-Bonnet term is included) and has no equivalent in four dimensions.

B. Quasinormal modes

The knowledge of the QNM frequencies of multidimensional BHs enables a clear physical interpretation of their gravitational emission. QNMs are free damped BH oscillations that are characterized by pure ingoing radiation at the BH horizon and pure outgoing radiation at infinity. The no-hair theorem implies that QNM frequencies depend only on the BH mass, charge, and angular momentum. Numerical simulations of BH collapse and BH-BH collision show that, after a transient phase depending on the details of the process, the newly formed BH has a *ringdown* phase, i.e., it undergoes damped oscillations that can be described as a superposition of slowly damped QNMs (modes with a small imaginary part). Furthermore, the QNMs determine the late-time evolution of perturbation fields in the BH exterior (for comprehensive reviews on QNMs see Refs. [38]).

Gravitational radiation from four-dimensional astrophysical BHs is dominated by slowly damped modes. In the following we show that these also dominate the emission of gravitational radiation in higher dimensions and determine important properties of the energy spectra. Recently, Konoplya computed slowly damped QNMs of higher-dimensional BHs [33,34] using the WKB method. This method is known to be inaccurate for large imaginary parts, but it is accurate enough for the slowly damped modes that are relevant in our context. Therefore, QNM frequencies for scalar, vector, and tensor gravitational perturbations are computed here in the WKB approximation. Our results are in good agreement with those presented by Konoplya in Ref. [34] (modulo a different normalization). At variance with Ref. [34], we concentrated on uncharged black holes in asymptotically flat, even-dimensional spacetimes. We extended Konoplya's calculation in two ways: (i) in addition to the fundamental QNM we also computed the first two overtones; (ii) we carried out our calculations for a much larger range of values of l (Ref. [34] only shows results for $l=2$ and $l=3$).

The method consists of applying the WKB approximation to the potential in Eq. (7) with appropriate boundary conditions. The result is a pair of connection formulas that relate the amplitudes of the waves on either side of the potential barrier, and ultimately yield an analytical formula for the QNM frequencies (for details see Refs. [39,40]). The WKB QNM frequencies ω^2 are given in terms of the potential maximum V_0 and of the potential derivatives at the maximum by

$$\omega^2 = (V_0 + \sqrt{-2V_0''}\Lambda) - i(j+\tfrac{1}{2})\sqrt{-2V_0''}(1+\Omega),$$

$$j=0,1,2,\ldots, \quad (15)$$

where

$$\Lambda = \frac{1}{\sqrt{-2V_0''}} \left[\frac{1}{8} \frac{V_0^{(4)}}{V_0''} \left(\frac{1}{4} + \alpha^2 \right) - \frac{1}{288} \left(\frac{V_0'''}{V_0''} \right)^2 (7+60\alpha^2) \right], \quad (16)$$

TABLE I. QNMs for $n=2$. The first three quasinormal frequencies for scalar and vector perturbations are listed from left to right. The scalar modes and the vector modes are isospectral in four dimensions.

$n=2$	Scalar and vector modes		
l	$j=0$	$j=1$	$j=2$
2	0.746-0.178i	0.692-0.550i	0.606-0.942i
3	1.199-0.185i	1.165-0.563i	1.106-0.953i
4	1.618-0.188i	1.593-0.569i	1.547-0.958i
5	2.025-0.190i	2.004-0.572i	1.967-0.960i
6	2.424-0.191i	2.407-0.573i	2.375-0.961i
7	2.819-0.191i	2.805-0.574i	2.777-0.961i
8	3.212-0.191i	3.200-0.575i	3.175-0.961i
9	3.604-0.192i	3.592-0.575i	3.570-0.962i
10	3.994-0.192i	3.983-0.576i	3.963-0.962i
11	4.383-0.192i	4.373-0.576i	4.355-0.962i
12	4.771-0.192i	4.762-0.576i	4.745-0.962i
13	5.159-0.192i	5.151-0.576i	5.135-0.962i
14	5.546-0.192i	5.539-0.577i	5.524-0.962i
15	5.934-0.192i	5.927-0.577i	5.913-0.962i

$$\Omega = \frac{1}{\sqrt{-2V_0''}}\left[\frac{5}{6912}\left(\frac{V_0'''}{V_0''}\right)^4(77+188\alpha^2) - \frac{1}{384}\left(\frac{V_0'''\,^2 V_0^{(4)}}{V_0''\,^3}\right)\right.$$

$$\times(51+100\alpha^2) + \frac{1}{2304}\left(\frac{V_0^{(4)}}{V_0''}\right)^2(67+68\alpha^2)$$

$$\left. + \frac{1}{288}\left(\frac{V_0'''V_0^{(5)}}{V_0''\,^2}\right)(19+28\alpha^2) - \frac{1}{288}\left(\frac{V_0^{(6)}}{V_0''}\right)(5+4\alpha^2)\right],$$

$$(17)$$

$\alpha=j+1/2$ and j is the mode index. The QNM frequencies for the scalar, vector, and tensor potentials of Sec. II and

various dimensions are shown in Tables I–IV and will be discussed in Sec. IV. Let us stress that the application of the WKB technique is questionable in a few higher-dimensional cases; for $l=2$ and $l=3$ the vector and scalar potentials in $D>6$ are not positive definite and/or display a second, small scattering peak close to the BH horizon. An accurate analysis of these potentials would require a refinement of the standard WKB technique, which is not presented here. These special cases are denoted by italic numbers in Tables III and IV.

We mention that highly damped QNMs of four- and higher-dimensional BHs have recently become a subject of great interest in a different context. A few years ago, Hod proposed to use Bohr's correspondence principle to determine the BH area quantum from highly damped BH QNMs [41]. Hod's proposal is quite general: the asymptotic QNM frequency for scalar perturbations of a nonrotating BH in D dimensions is the same as in four dimensions [42]. Quite notably, this result holds also for scalar, vector, and tensor gravitational perturbations [43,42]. Reference [44] contains a partial list of references on recent developments in this field.

III. INTEGRATION METHOD

The computation of the gravitational wave emission of an ultrarelativistic particle plunging into a BH requires the numerical integration of the inhomogeneous wave equation for scalar gravitational perturbations. (Vector and tensor gravitational perturbations are not excited by a particle in radial infall.) The source term $S^{(n)}$ for the corresponding wave equation in $n+2$ dimensions can be calculated from the stress-energy tensor of the infalling particle. Details of the derivation are in Appendix A.

The integration in $(n+2)$ dimensions proceeds as in four dimensions [19,20]. A good summary of the integration procedure can be found in Ref. [22]. In this section we simply stress the differences between the four- and the $(n+2)$-dimensional cases. For the sake of simplicity, in our

TABLE II. QNMs for $n=4$. The first three quasinormal frequencies for scalar, vector, and tensor perturbations are listed from right.

$n=4$	Scalar modes			Vector modes			Tensor modes		
l	$j=0$	$j=1$	$j=2$	$j=0$	$j=1$	$j=2$	$j=0$	$j=1$	$j=2$
2	1.131-0.386i	0.922-1.186i	0.537-2.053i	1.543-0.476i	1.279-1.482i	0.825-2.583i	2.004-0.503i	1.764-1.568i	1.378-2.732i
3	1.915-0.399i	1.715-1.217i	1.336-2.103i	2.191-0.471i	1.988-1.445i	1.625-2.492i	2.576-0.499i	2.393-1.531i	2.075-2.632i
4	2.622-0.438i	2.476-1.331i	2.208-2.271i	2.824-0.474i	2.664-1.441i	2.369-2.460i	3.146-0.498i	2.998-1.514i	2.729-2.580i
5	3.279-0.457i	3.156-1.384i	2.924-2.347i	3.441-0.478i	3.310-1.447i	3.063-2.453i	3.716-0.497i	3.592-1.504i	3.359-2.549i
6	3.911-0.467i	3.803-1.412i	3.598-2.385i	4.046-0.481i	3.935-1.453i	3.723-2.454i	4.286-0.496i	4.179-1.498i	3.974-2.530i
7	4.527-0.474i	4.432-1.429i	4.249-2.408i	4.644-0.484i	4.547-1.458i	4.360-2.456i	4.856-0.496i	4.762-1.495i	4.580-2.517i
8	5.133-0.478i	5.048-1.441i	4.883-2.422i	5.236-0.485i	5.150-1.462i	4.983-2.458i	5.427-0.495i	5.342-1.492i	5.178-2.508i
9	5.732-0.481i	5.655-1.449i	5.505-2.432i	5.824-0.487i	5.747-1.466i	5.596-2.460i	5.997-0.495i	5.921-1.490i	5.772-2.501i
10	6.326-0.484i	6.256-1.455i	6.118-2.439i	6.409-0.488i	6.339-1.468i	6.201-2.462i	6.567-0.495i	6.498-1.489i	6.361-2.496i
11	6.916-0.485i	6.852-1.459i	6.725-2.444i	6.992-0.489i	6.928-1.470i	6.801-2.463i	7.138-0.495i	7.074-1.488i	6.948-2.492i
12	7.504-0.487i	7.444-1.463i	7.326-2.448i	7.574-0.490i	7.514-1.472i	7.396-2.464i	7.708-0.495i	7.649-1.487i	7.532-2.489i
13	8.088-0.488i	8.033-1.465i	7.923-2.452i	8.153-0.490i	8.098-1.473i	7.988-2.465i	8.279-0.495i	8.224-1.486i	8.115-2.487i
14	8.671-0.489i	8.619-1.468i	8.517-2.454i	8.732-0.491i	8.680-1.474i	8.577-2.465i	8.849-0.495i	8.798-1.486i	8.696-2.485i
15	9.253-0.489i	9.204-1.469i	9.108-2.456i	9.309-0.491i	9.261-1.475i	9.164-2.466i	9.420-0.495i	9.371-1.485i	9.275-2.483i

TABLE III. QNMs for $n=6$. The first three quasinormal frequencies for scalar, vector, and tensor perturbations are listed from left to right. The numbers in italic indicate that the potential at the given l is not everywhere positive definite. The square brackets indicate that the potential has two scattering peaks.

$n=4$	Scalar modes			Vector modes			Tensor modes		
l	$j=0$	$j=1$	$j=2$	$j=0$	$j=1$	$j=2$	$j=0$	$j=1$	$j=2$
2	*[1.778-0.571i]*	*[1.289-1.770i]*	*[0.395-3.201i]*	2.388-0.720i	*1.831-2.237i*	*0.825-4.001i*	2.956-0.751i	2.365-2.357i	1.339-4.245i
3	2.604-0.628i	2.198-1.916i	1.403-3.355i	3.102-0.715i	2.660-2.191i	1.814-3.833i	3.623-0.747i	3.181-2.294i	2.351-4.012i
4	3.401-0.645i	3.050-1.958i	2.346-3.375i	3.815-0.712i	3.450-2.165i	2.730-3.731i	4.282-0.744i	3.926-2.264i	3.235-3.895i
5	4.174-0.660i	3.875-1.997i	3.270-3.403i	4.522-0.712i	4.213-2.156i	3.595-3.678i	4.940-0.741i	4.640-2.247i	4.047-3.830i
6	4.923-0.675i	4.665-2.037i	4.144-3.449i	5.222-0.714i	4.954-2.156i	4.418-3.654i	5.598-0.740i	5.337-2.236i	4.818-3.789i
7	5.653-0.687i	5.425-2.070i	4.967-3.492i	5.915-0.716i	5.679-2.160i	5.207-3.645i	6.255-0.739i	6.024-2.229i	5.563-3.763i
8	6.369-0.695i	6.164-2.095i	5.753-3.525i	6.602-0.719i	6.392-2.164i	5.969-3.643i	6.913-0.738i	6.705-2.224i	6.290-3.745i
9	7.075-0.702i	6.888-2.113i	6.515-3.550i	7.285-0.721i	7.094-2.169i	6.712-3.644i	7.570-0.738i	7.382-2.221i	7.004-3.732i
10	7.772-0.707i	7.602-2.128i	7.259-3.570i	7.964-0.722i	7.790-2.173i	7.441-3.646i	8.228-0.737i	8.055-2.218i	7.709-3.722i
11	8.464-0.711i	8.306-2.139i	7.989-3.585i	8.640-0.724i	8.480-2.177i	8.158-3.648i	8.885-0.737i	8.726-2.216i	8.406-3.715i
12	9.151-0.715i	9.004-2.148i	8.709-3.598i	9.314-0.725i	9.165-2.180i	8.867-3.650i	9.543-0.737i	9.395-2.215i	9.098-3.709i
13	9.834-0.717i	9.697-2.156i	9.421-3.607i	9.986-0.726i	9.847-2.183i	9.569-3.653i	10.200-0.737i	10.062-2.214i	9.785-3.705i
14	10.51-0.720i	10.39-2.162i	10.13-3.616i	10.66-0.727i	10.53-2.185i	10.27-3.655i	10.86-0.737i	10.73-2.213i	10.47-3.701i
15	11.19-0.721i	11.07-2.167i	10.83-3.622i	11.32-0.728i	11.20-2.187i	10.96-3.657i	11.52-0.736i	11.39-2.212i	11.15-3.698i

numerical integrations we set the horizon radius $r_h = (2M)^{1/(n-1)} = 1$. The equation for the scalar perturbations is

$$\left(\frac{d^2}{dr_*^2} + \omega^2 - V_S \right) \Phi = S^{(n)}. \qquad (18)$$

The general solution of Eq. (18) is obtained via a Green function technique as follows. Consider two independent (*left* and *right*) solutions of the homogeneous equation with boundary conditions $\Phi_L \sim e^{-i\omega r_*}$ for $r_* \to -\infty$, and $\Phi_R \sim e^{i\omega r_*}$ for $r_* \to +\infty$. For $r_* \to +\infty$ the left solution is a superposition of ingoing and outgoing waves of the form

$$\Phi_L \sim B(\omega)e^{i\omega r_*} + C(\omega)e^{-i\omega r_*}. \qquad (19)$$

The Wronskian is given by $W = 2i\omega C(\omega)$. The wave amplitude is obtained from a convolution of the left solution with the source term

$$\Phi = \frac{1}{W} \int_{-\infty}^{+\infty} \Phi_L S^{(n)} dr_*. \qquad (20)$$

The energy spectrum can be expressed in terms of the wave amplitude as (details of the derivation are given in Appendix B)

TABLE IV. QNMs for $n=8$. The first three quasinormal frequencies for scalar, vector, and tensor perturbations are listed from left to right. The numbers in italic indicate that the potential at the given l is not everywhere positive definite. The square brackets indicate that the potential has two scattering peaks.

$n=4$	Scalar modes			Vector modes			Tensor modes		
l	$j=0$	$j=1$	$j=2$	$j=0$	$j=1$	$j=2$	$j=0$	$j=1$	$j=2$
$l=2$	*[2.513-0.744i]*	*[1.686-2.299i]*	*[0.159-4.345i]*	3.261-0.924i	*2.335-2.851i*	*0.598-5.287i*	3.886-0.959i	2.765-2.988i	0.706-5.720i
$l=3$	*[3.388-0.812i]*	*[2.696-2.461i]*	*[1.277-4.431i]*	*4.017-0.923i*	*3.269-2.804i*	*1.747-5.016i*	4.618-0.959i	3.806-2.917i	2.141-5.241i
$l=4$	4.223-0.841i	3.631-2.532i	2.367-4.420i	4.775-0.920i	4.147-2.777i	2.824-4.840i	5.336-0.955i	4.691-2.885i	3.331-5.018i
$l=5$	5.042-0.855i	4.524-2.568i	3.407-4.401i	5.531-0.918i	4.991-2.762i	3.840-4.734i	6.049-0.951i	5.507-2.866i	4.360-4.904i
$l=6$	5.848-0.865i	5.390-2.595i	4.403-4.399i	6.283-0.917i	5.810-2.757i	4.802-4.676i	6.761-0.949i	6.291-2.854i	5.297-4.838i
$l=7$	6.640-0.874i	6.231-2.622i	5.357-4.415i	7.030-0.918i	6.610-2.757i	5.719-4.646i	7.473-0.947i	7.056-2.846i	6.178-4.798i
$l=8$	7.420-0.883i	7.052-2.647i	6.270-4.441i	7.774-0.920i	7.396-2.759i	6.599-4.634i	8.184-0.946i	7.808-2.841i	7.022-4.772i
$l=9$	8.191-0.890i	7.855-2.669i	7.149-4.469i	8.514-0.921i	8.167-2.764i	7.450-4.630i	8.895-0.945i	8.553-2.837i	7.841-4.755i
$l=10$	8.953-0.896i	8.645-2.688i	7.999-4.495i	9.250-0.923i	8.935-2.768i	8.278-4.630i	9.606-0.944i	9.292-2.834i	8.640-4.743i
$l=11$	9.709-0.902i	9.423-2.705i	8.829-4.519i	9.984-0.924i	9.692-2.773i	9.088-4.633i	10.32-0.944i	10.03-2.832i	9.426-4.735i
$l=12$	10.46-0.906i	10.19-2.718i	9.641-4.539i	10.71-0.926i	10.44-2.777i	9.884-4.637i	11.03-0.943i	10.76-2.831i	10.20-4.728i
$l=13$	11.20-0.910i	10.95-2.730i	10.44-4.556i	11.44-0.927i	11.19-2.781i	10.67-4.642i	11.74-0.943i	11.49-2.829i	10.97-4.724i
$l=14$	11.95-0.914i	11.71-2.740i	11.23-4.571i	12.17-0.928i	11.93-2.785i	11.44-4.646i	12.45-0.943i	12.21-2.828i	11.73-4.720i
$l=15$	12.68-0.916i	12.46-2.748i	12.01-4.584i	12.90-0.929i	12.67-2.788i	12.21-4.650i	13.16-0.943i	12.94-2.828i	12.48-4.718i

$$\frac{dE}{d\omega} = \frac{\omega^2}{16\pi} \frac{n-1}{n} \kappa^2 (\kappa^2 - n) |\Phi|^2, \tag{21}$$

where $\kappa^2 \equiv l(l+n-1)$. The Wronskian for a given value of ω is obtained by integrating the homogeneous equation from

a point located as close as possible to the horizon, and expanding Φ_L as

$$\Phi_L \sim e^{-i\omega r}* [1 + a_{n+2}(r-1) + \dots], \tag{22}$$

where

$$a_{n+2} = \frac{-(l^4 + 2l^3 - l^2 - 2l + 3) + (n-2)[-2l^3 + l^2 + (n^2+1)l - (n^3 + 4n^2 + n + 6)/4]}{(2i\omega - 1)(l^2 + l + 1) + (n-2)[-l^2 + (2i\omega - n)l + (n+1)i\omega - (n^2+1)/2]}. \tag{23}$$

$C(\omega)$ (and W) can be obtained with good accuracy by matching the numerically integrated Φ_L to the asymptotic expansion

$$\Phi_L \sim e^{i\omega r}* \left[1 + \frac{a_{n+2}(\omega)}{r} + \frac{b_{n+2}(\omega)}{r^2} + \dots \right]$$
$$+ e^{-i\omega r}* \left[1 + \frac{a_{n+2}(-\omega)}{r} + \frac{b_{n+2}(-\omega)}{r^2} + \dots \right], \tag{24}$$

where the leading-order coefficient is

$$a_{n+2}(\omega) = \frac{i[l^2 + (n-1)l + n(n-2)/4]}{2\omega}. \tag{25}$$

For given n, l, and ω, the error on the Wronskian and on the energy spectrum is typically of the order of $O(10^{-4})$.

IV. RESULTS

The main results of our work are the computation of the QNM frequencies in the WKB approximation, the computation of the energy spectra, and the estimate of the total energy and angular distribution of the radiation emitted during the plunge. These results are discussed in detail below.

A. Quasinormal frequencies

The WKB QNM frequencies for different even values of n are listed in Tables I–IV. Each line shows the first three quasinormal frequencies ($j=0,1,2$) for scalar, vector, and tensor perturbations at given l. For $n=2$ tensor perturbations do not exist. In this case the scalar and vector entries correspond to the QNMs of the Zerilli and Regge-Wheeler equations, which are known to be isospectral [21]. The isospectrality is broken for $n>2$. This has been shown analytically by Kodama and Ishibashi [30] and later verified numerically by Konoplya [34]. The real and imaginary parts of scalar QNM frequencies at given n, l, and j are smaller than those of vector QNMs, which are in turn smaller than those of tensor QNMs. Since scalar modes are the least damped, they are likely to dominate the gravitational radiation emission.

As l grows, the isospectrality tends to be restored. In the eikonal limit $l \to \infty$ the centrifugal term of the potential dominates and is the same for scalar, vector, and tensor perturbations. In this limit, the QNM frequencies for all perturbations are

$$\omega_R \sim \frac{n+2l-1}{2} \left(\frac{2}{n+1} \right)^{1/(n-1)} \left(\frac{n-1}{n+1} \right)^{1/2},$$

$$\omega_I \sim \frac{n-1}{2(n+1)^{1/2}} \left(\frac{2}{n+1} \right)^{1/(n-1)} (2j+1). \tag{26}$$

The previous relation was derived in Ref. [33] for multidimensional BH perturbations induced by a scalar field. (Notice that the normalization used in Ref. [33] is different from ours.) Here we have shown that it also holds for gravitational perturbations. Isospectrality of scalar and gravitational perturbations is a common feature of the eikonal limit and of the large-damping limit [42,43] for any n.

B. Multipolar components of the energy spectra

The numerical integration described in Sec. III gives the energy spectra of Figs. 1 and 2. The spectra for $n=2$ (top left panel in Fig. 1) are in excellent agreement with those of Ref. [22]. The spectra are flat in the region between the zero-frequency limit and a "cutoff" frequency ω_c, beyond that they fall exponentially to zero. The cutoff frequency ω_c is given by the fundamental QNM frequency to a good level of accuracy. This result can be understood in terms of gravitational-wave scattering from the potential barrier that surrounds the black hole. ω^2 plays the role of the energy in the Schrödinger-like equation (7). From Eq. (15) it follows that $\omega^2 = V_0$ at first order in the WKB approximation. Therefore, only the radiation with energy smaller than the peak of the potential is backscattered to infinity; radiation with larger frequency is exponentially suppressed.

The gravitational emission of a two-particle hard collision in higher dimensions has been computed by Cardoso *et al.* [25] using techniques developed in four dimensions by Weinberg [45] and later used by Smarr [24]. The main result of Ref. [25] is that the spectra in $n+2$ dimensions grow as ω^{n-2}; thus the integrated spectra diverge as ω^{n-1}. Physically meaningful results for the total energy can only be obtained by imposing some cutoff on the integrated spectra.
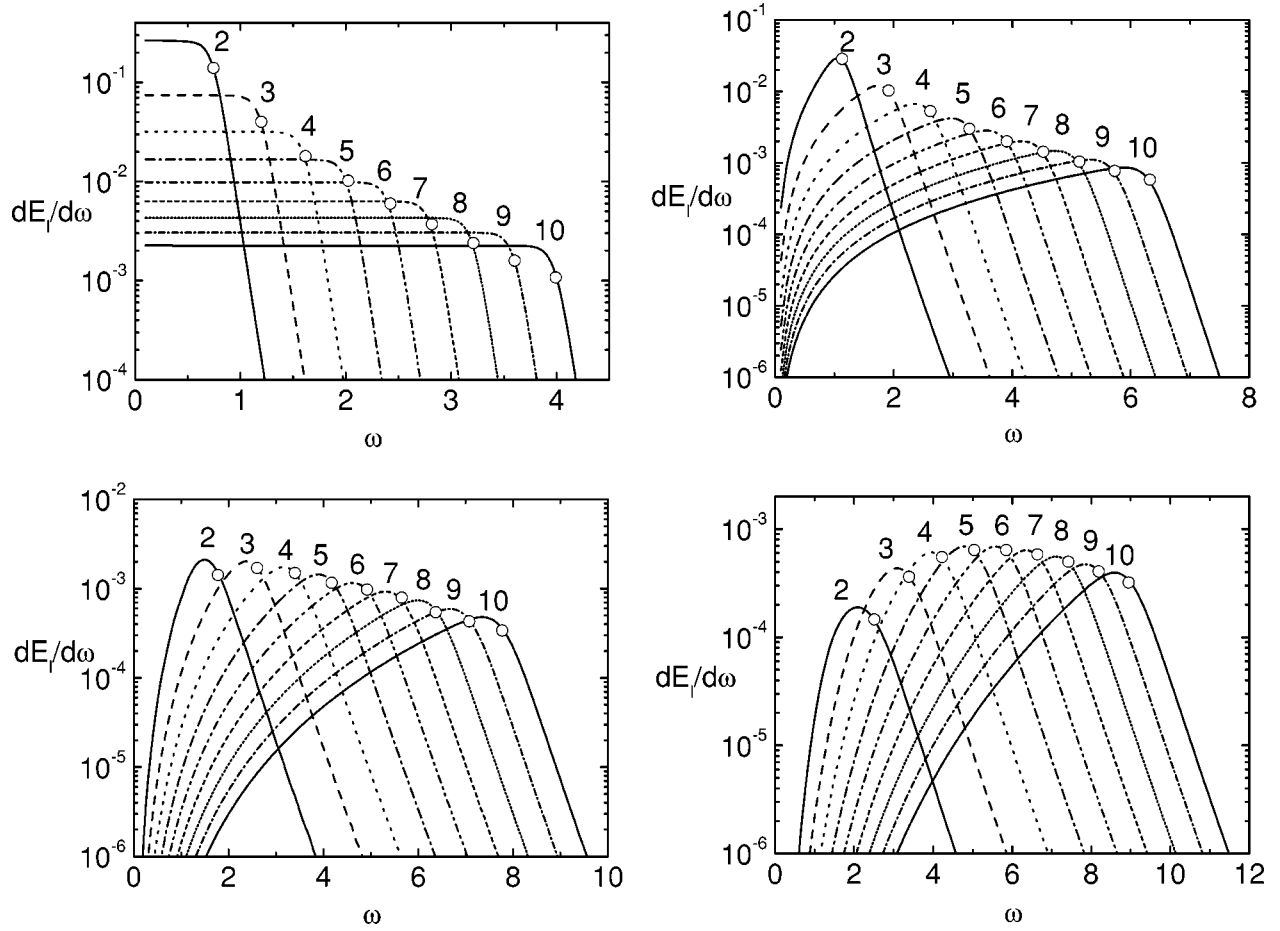
FIG. 1. Multipolar components of the energy spectra up to $l = 10$ for $n = 2$, $n = 4$ (top left and top right panels), $n = 6$ and $n = 8$ (bottom left and bottom right panels) in units $r_h = 1$. Open circles mark the real part of the fundamental scalar gravitational quasinormal frequency, ω_{ln}, for the given l and n.

Smarr [24] first suggested to use the inverse horizon radius as a cutoff. The relativistic perturbative calculation in $n = 2$ [22] shows that the cutoff frequency at fixed l is very close to the fundamental BH QNM. Therefore, the cutoff frequency

should be given by some "weighted average" of the fundamental gravitational QNM frequencies [25].

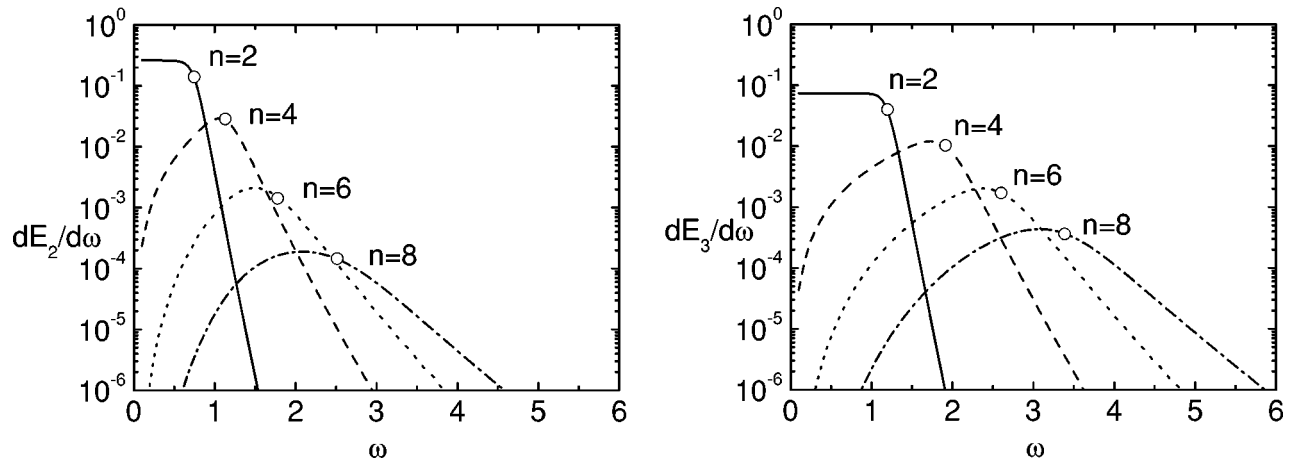Our results for the spectra and the QNMs confirm the above picture. Figure 1 shows that all spectra go to zero as

FIG. 2. Multipolar components of the energy spectra at fixed l for different values of n in units $r_h = 1$. The left panel corresponds to $l = 2$ and the right panel corresponds to $l = 3$. Open circles mark the real part of the fundamental scalar gravitational quasinormal frequency, ω_{ln}, for the given l and n.

BERTI, CAVAGLIÀ, AND GUALTIERI

PHYSICAL REVIEW D **69**, 124011 (2004)

$\omega \to 0$. For $\omega < \omega_c$ the spectrum at fixed l is

$$\frac{dE_l}{d\omega} = f_{n,l}\omega^{n-2}, \tag{27}$$

where $f_{n,l}$ is a constant that can be found by a fit of the spectra. For large l $f_{n,l}$ decays as

$$f_{n,l} = k_{n+2}l^{-3(n+2)/4}. \tag{28}$$

A fit of the numerical data gives $k_4 = 2.25$, $k_6 = 0.832$, $k_8 = 0.184$, and $k_{10} = 0.040$. Our result for $n=2$ is consistent with that of Ref. [22].

As conjectured in Ref. [25], all spectra have a maximum at some cutoff frequency ω_c. This cutoff frequency is very close to the fundamental QNM frequency ω_{ln} for (scalar) gravitational perturbations with given l and n, which is marked by open circles in Figs. 1 and 2. The deviation between ω_c and ω_{ln} is of order 10% for low l, and decreases for large l (compare Figs. 1 and 2 to the first column of Tables I–IV). The deviation is larger when the WKB method is least reliable, namely for $l=2$ and $n>4$. In these cases, the location of the peaks in the spectra can presumably be used as a more reliable estimate of the QNM frequency. The spectrum decays exponentially for $\omega > \omega_c$ with an n-dependent slope α_{n+2} (see Fig. 2):

$$\frac{dE_l}{d\omega} \sim e^{-\alpha_{n+2}(\omega - \omega_c)}. \tag{29}$$

Thus the ω-integrated multipolar contributions ΔE_l at given l are finite. With our choice of units, Cardoso and Lemos [22] find $\alpha_4 = 13.5\alpha$ (here α is a constant of order unity that cannot easily be determined because the spectra decay very quickly). Our numerical fits give $\alpha_4 \simeq 15$, in good agreement with their result. In higher dimensions the constants α_{n+2} are comparatively easier to determine. Their values are $\alpha_6 \simeq 5.5$, $\alpha_8 \simeq 3.4$, and $\alpha_{10} \simeq 2.3$. It is not clear if there is any relation between this n-dependent slope and the late-time tail behavior predicted in Ref. [26].

Figure 1 shows that higher multipoles contribute more as n grows. This is evident when we look at the ω-integrated multipolar components of the energy spectra of Fig. 3. The quadrupole ($l=2$) is dominant only for $n=2$ and $n=4$. For $n=6$ and $n=8$ the dominant multipoles are $l=4$ and $l=6$, respectively (see Table V). This effect may be related to the appearance of a negative well in the scalar potentials for $l=2$ and $n>4$. It would be interesting to understand better the physical relation between the dominant multipole and the spacetime dimension.

C. Total energy

The total emitted energy is obtained by numerically integrating the results of the previous section over ω and summing the multipolar components. For large l the integrated energy in the multipole l can be fitted by

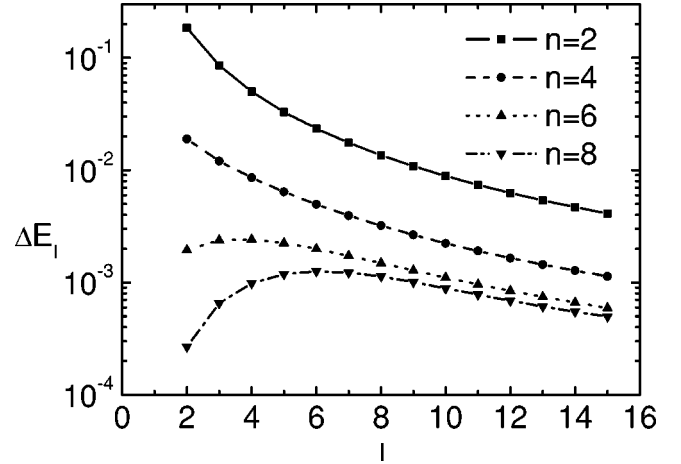$$\Delta E_l = a_{n+2}l^{-b_{n+2}}, \tag{30}$$

FIG. 3. The integrated energy ΔE_l as a function of l for different values of n. The dominant multipolar component is $l=2$ only for $n<6$; this is probably related to the appearance of a negative well in the scalar potentials for $l=2$ and $n>4$. The dominant multipole is $l=4$ (6) for $n=6$ (8) (see Table V).

where $(a_6 = 0.110, b_6 = 1.69)$, $(a_8 = 0.050, b_8 = 1.64)$, and $(a_{10} = 0.022, b_{10} = 1.40)$ for $n=4$, $n=6$, and $n=8$, respectively. The coefficients (a_{n+2}, b_{n+2}) have been obtained by fitting the data from $l=14$ to $l=20$ and are weakly dependent on the chosen range of l. This variability affects our final results on the total energy within less than a few percent.

Restoring the dependence on the BH horizon r_h and on the conserved particle energy p_0, the total emitted energy is

$$E_{\rm em} = \frac{p_0^2}{M_{\rm BH}}\frac{n\mathcal{A}_n}{16\pi}\sum_{l=2}^{\infty}\Delta E_l \equiv \frac{p_0^2}{M_{\rm BH}}\frac{n\mathcal{A}_n}{16\pi}E_{\rm tot}^{(D)} \equiv \frac{p_0^2}{M_{\rm BH}}\mathcal{E}_{\rm tot}^{(D)}, \tag{31}$$

where $E_{\rm tot}^{(D)}$ is the "dimensionless" total energy (expressed in the units $r_h = 1$ that we used in our numerical integrations).

TABLE V. Multipolar contributions to the total energy for different n in units $r_h = 1$.

l	$n=2$	$n=4$	$n=6$	$n=8$
2	0.1845	0.189×10^{-1}	0.194×10^{-2}	0.269×10^{-3}
3	0.0855	0.120×10^{-1}	0.238×10^{-2}	0.653×10^{-3}
4	0.0500	0.086×10^{-1}	0.241×10^{-2}	0.983×10^{-3}
5	0.0329	0.064×10^{-1}	0.224×10^{-2}	1.187×10^{-3}
6	0.0234	0.050×10^{-1}	0.199×10^{-2}	1.258×10^{-3}
7	0.0175	0.039×10^{-1}	0.172×10^{-2}	1.225×10^{-3}
8	0.0136	0.032×10^{-1}	0.149×10^{-2}	1.130×10^{-3}
9	0.0109	0.027×10^{-1}	0.128×10^{-2}	1.009×10^{-3}
10	0.0089	0.022×10^{-1}	0.111×10^{-2}	0.888×10^{-3}
11	0.0074	0.019×10^{-1}	0.096×10^{-2}	0.780×10^{-3}
12	0.0063	0.016×10^{-1}	0.084×10^{-2}	0.688×10^{-3}
13	0.0054	0.014×10^{-1}	0.075×10^{-2}	0.612×10^{-3}
14	0.0047	0.013×10^{-1}	0.066×10^{-2}	0.549×10^{-3}
15	0.0041	0.011×10^{-1}	0.059×10^{-2}	0.497×10^{-3}

124011-8

TABLE VI. Total energy for different spacetime dimensions. From left to right, the columns give the spacetime dimension $D = n+2$, the factor $n\mathcal{A}_n/16\pi$, the total energy $E_{\mathrm{tot}}^{(D)}$ in units $r_h = 1$, the rescaled total energy $\mathcal{E}_{\mathrm{tot}}^{(D)} = n\mathcal{A}_n E_{\mathrm{tot}}^{(D)}/16\pi$ and the gravitational energy loss (see text).

D	$n\mathcal{A}_n/16\pi$	$E_{\mathrm{tot}}^{(D)}$	$\mathcal{E}_{\mathrm{tot}}^{(D)}$	Energy loss
4	$1/2$	0.52	0.26	13%
6	$2\pi/3$	0.095	0.20	10%
8	$2\pi^2/5$	0.034	0.13	7%
10	$16\pi^3/105$	0.032	0.15	8%

We obtained the integrated spectra numerically up to $l = 20$ and extrapolated them for larger l using the fits in Eq. (30). Results are presented in Table VI.

Following Ref. [22] we estimate the gravitational energy loss for a collision of two particles with equal mass M by the replacement $p_0 \to M$, $M_{\mathrm{BH}} \to M_{\mathrm{tot}} = 2M$. For $n=2$ this extrapolation gives results in good agreement with the perturbative shock-wave calculation of Ref. [12], which considers two BHs of equal mass. An analogous extrapolation for $n = 2$ gives results in close agreement with the fully relativistic computation [16] for a particle starting from infinity at rest. Therefore, we believe that our extrapolation should provide a qualitative but realistic estimate. The results for different values of n are given in the last column of Table VI. The gravitational energy loss is $\sim 13\%$, $\sim 10\%$, 7%, and 8% for $n = 2$ to $n = 8$, respectively. The result for $n = 2$ is in good agreement with previous estimates [12] (see the discussion in Ref. [22]).

D. Angular dependence

The angular dependence of the radiation is obtained by evaluating numerically Eqs. (B17) and (B18). Figure 4 shows the angular dependence of the total energy up to $l = 15$ for $n = 2$, $n = 4$, and $n = 6$.
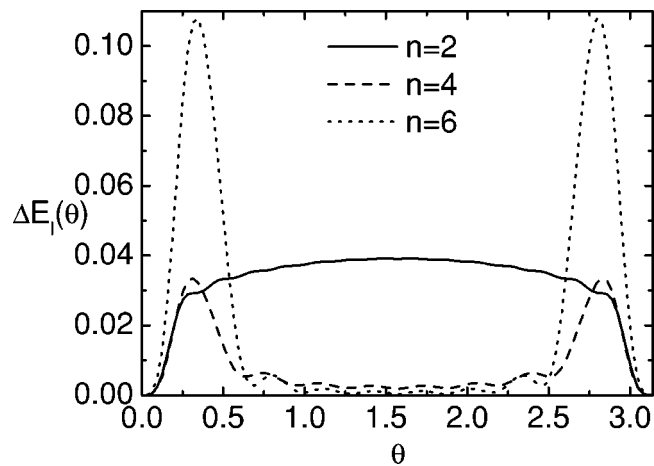

FIG. 4. Angular dependence of the radiation for $n = 2$, 4, and 6, summing all multipoles up to $l = 15$ in units $r_h = 1$. The angular distribution for $n = 8$ is not shown. The latter is even more peaked in a narrow region around $\theta = 0$ since also the multipoles with $l > 15$ contribute significantly to the radiation.

The angular distribution of the gravitational radiation in the BH frame goes to zero along the axis of the collision ($\theta = 0, \pi$) in any dimensions. Therefore, the gravitational emission is never back- or forward scattered. In four dimensions the angular spectrum of the gravitational radiation increases rapidly at small θ and becomes approximately flat at greater angles with a maximum in the direction orthogonal to the axis of the collision, before falling rapidly to zero for values of the angles close to π. The angular distribution of the gravitational radiation for $n > 2$ is peaked at θ and $\pi - \theta$, where θ is a small angle. The difference between the behavior of the angular distribution in four dimensions and in higher dimensions has no evident physical reason. It would be interesting to further explore this point.

V. CONCLUSION AND PERSPECTIVES

In this paper we have computed the gravitational emission of a two-particle collision in an even D-dimensional spacetime. We have presented the numerical results for $D = 4$ to 10. The collision has been modeled as a massless test particle plunging into a BH with mass equal to the c.m. energy of the event.

According to our estimates, the total emitted energy in a head-on collision with particles of equal mass ranges from $\sim 13\%$ ($D=4$) to $\sim 8\%$ ($D=10$). This shows that the loss in gravitational radiation is quite stable under variation of the spacetime dimension and slightly decreases for higher D. The result for $D=4$ confirms previous numerical and analytical calculations [12].

Our result contrasts with the YN estimation for the initial mass of a BH in head-on collisions [10]. A possible explanation is that the junk emission is not wholly gravitational emission. The YN method predicts the mass within the apparent horizon to be $\sim 0.71 E_{\mathrm{cm}}$ in four dimensions. If all the junk energy were gravitational radiation, this would amount to a total loss of around 30%. The disagreement is likely not due to numerical uncertainties or inaccurate approximations: the YN mass decreases for higher spacetime dimensions ($\sim 0.71 E_{\mathrm{cm}}$ to $\sim 0.58 E_{\mathrm{cm}}$ for $D=4$ to $D=11$), whereas the loss in gravitational radiation remains stable. Since both YN and our methods are purely gravitational, this "dark component" of the junk radiation should describe the by-products of the collision. According to this picture, $\sim 60\%$ of the c.m. energy in ten dimensions is trapped inside the horizon, $\sim 10\%$ is emitted in gravitational radiation, and $\sim 30\%$ goes into particle by-products in the final state. These could be the carriers of the initial charge in a collision between charged particles. For $D>4$ a fraction of the by-products may be emitted into the bulk.

Let us conclude by briefly discussing the phenomenological consequences of these results for BH formation at the TeV scale. Although uncertainties may affect the numerical estimates, different approaches now confirm that some of the initial c.m. energy is not trapped inside the BH horizon. For head-on collisions in $D=10$, for example, this junk energy ranges from $\sim 10\%$ (optimistic value—our result) to $\sim 40\%$ (pessimistic value—YN result). Hence, the initial mass of the BH formed in the collision could be considerably smaller

than the c.m. energy. The experimental signatures of BH production at particle colliders and in ultrahigh energy cosmic ray events strongly depend on the initial BH mass. The total multiplicity of the Hawking phase in ten dimensions could be almost halved in the pessimistic case, leading to a greater average energy of the emitted quanta.

A thorough investigation of the effects of energy loss in TeV-scale BH production is undoubtedly worth pursuing. Future research should focus on the extension of the above results to spacetimes with odd dimensions and to gravitational events with different geometries. BHs produced in colliders, for instance, possess nonvanishing angular momentum. Rotating BHs are expected to lose more energy in gravitational waves than Schwarzschild BHs of equal mass. A larger gravitational emission is also expected for non-spherically symmetric BHs. This is particularly relevant when the compactified space is asymmetric, and some of the extra dimensions have size of order of the fundamental gravitational scale. It would be extremely important to quantify these differences.

ACKNOWLEDGMENTS

APPENDIX A: THE SOURCE TERM

In this appendix we derive the source term of the KI equation that describes the radial plunge of a massless particle into the $(n+2)$-dimensional BH. The perturbation of the stress-energy tensor is

$$\delta T^{\mu\nu} = -\frac{p_0}{\sqrt{-g}} \int d\lambda \, \delta^n(x - x(\lambda)) \frac{dx^\mu}{d\lambda} \frac{dx^\nu}{d\lambda}, \quad \text{(A1)}$$

where p_0 is the conserved energy of the particle. The only nonvanishing components of the particle velocity are u^t and u^r. Thus the source excites only scalar perturbations. Following the notations of Ref. [29], Eq. (A1) reads

$$\delta T_{\mu\nu} = \left(\begin{array}{c|c} \tau_{ab}\mathcal{S} & 0 \\ \hline 0 & 0 \end{array} \right), \quad \text{(A2)}$$

where $\mathcal{S}$ are the scalar harmonics and τ_{ab} are the nonvanishing gauge-invariant perturbations of the stress-energy tensor. The BH+source system is symmetric under rotation of the $(n-1)$-sphere S^{n-1} [46]. Consequently, the harmonic decomposition of the fields contains only harmonics invariant under S^{n-1}. We can write the metric of S^n as

$$d\Omega_n(\theta, \phi_1, \ldots, \phi_{n-1}) = d\theta^2 + \sin^2\theta \, d\Omega_{n-1}(\phi_1, \ldots, \phi_{n-1})$$
$$\text{(A3)}$$

and choose the trajectory of the test particle to be $\theta = 0$. The harmonics which are invariant under S^{n-1} do not depend on $\phi_1, \ldots, \phi_n$. The scalar harmonics on S^n belong to the representations $D^{(l)}$ of $SO(n+1)$

$$D^{(l)} = \underbrace{\boxed{\begin{array}{|c|c|c|} \hline & \cdots & \\ \hline \end{array}}}_{l}. \quad \text{(A4)}$$

Each harmonic is labeled by the index l denoting its representation and by additional indices in the representation. We fix a particular element of each representation $D^{(l)}$ [the singlet under $SO(n-1)$] by requiring the harmonics to be invariant under S^{n-1}. Therefore, the harmonics in the expansion of the perturbations depend only on l and on the dimension n of the sphere. A $(n+2)$-dimensional scalar field can then be expanded as [46]

$$\phi(t, r, \theta, \phi_1, \ldots, \phi_{n-1}) = \sum_l \tilde{\phi}_l(t, r) \mathcal{S}^{(nl)}(\theta), \quad \text{(A5)}$$

where $\mathcal{S}^{(nl)}(\theta)$ satisfy

$$D_i D^i \mathcal{S}^{(nl)} = -\kappa^2 \mathcal{S}^{(nl)}, \quad \kappa^2 \equiv l(l+n-1), \quad \text{(A6)}$$

and

$$\int d\Omega_n \mathcal{S}^{(nl)} \mathcal{S}^{*(nl')} = \delta_{ll'}. \quad \text{(A7)}$$

The solution of Eq. (A6) is

$$\mathcal{S}^{(nl)}(\theta) = K^{(nl)} C_l^{(n-1)/2}(\theta), \quad \text{(A8)}$$

where $C_l^{(n-1)/2}(\theta)$ are Gegenbauer polynomials [47] and $K^{(nl)}$ are normalization factors. Using Eq. (A7) we have

$$K^{(nl)}$$

$$= \left[\frac{2^{3-n}\pi^{n/2+1}}{\Gamma(n/2)} \frac{\Gamma(l+n-1)}{(l+n/2-1/2)\Gamma(n/2-1/2)^2\Gamma(l+1)} \right]^{-1/2}.$$
$$\text{(A9)}$$

The scalar harmonics for the source are obtained setting $\theta = 0$:

$$S^{(nl)}(\theta=0) = K^{(nl)} \frac{(l+n-2)!}{(n-2)!l!}. \quad \text{(A10)}$$

For a massive particle in radial geodesic motion

$$\frac{dt}{dr} = -\frac{1}{f(r)}. \quad \text{(A11)}$$

From Eqs. (A11) and (4) it follows that

$$r_*(r) = -t(r), \tag{A12}$$

where we have set to zero the integration constant. The stress-energy tensor perturbations are

$$\delta T_{rr}(t,r,\theta,\phi_1,\dots) = -p_0 f^{-2} r^{-n} \delta(t-t(r)) \delta^n(\Omega_n),$$

$$\delta T_{tr}(t,r,\theta,\phi_1,\dots) = -p_0 f^{-1} r^{-n} \delta(t-t(r)) \delta^n(\Omega_n). \tag{A13}$$

(δT_{tt} does not contribute to the source of the KI equation.) Integrating Eqs. (A13) on S^n and applying a Fourier transform, the gauge-invariant perturbations are

$$\tau_{rr}(\omega,r) = -p_0 f^{-2} r^{-n} \frac{e^{i\omega t(r)}}{\sqrt{2\pi}} S^{(nl)}(\theta=0),$$

$$\tau_{tr}(\omega,r) = -p_0 f^{-1} r^{-n} \frac{e^{i\omega t(r)}}{\sqrt{2\pi}} S^{(nl)}(\theta=0). \tag{A14}$$

The source term $S^{(n)}$ for scalar gravitational perturbations is obtained in terms of τ_{ab} by substituting Eqs. (A14) in Eq. (5.44) of Ref. [32], where

$$S_{ab} = 8\pi r^{n-2} \tau_{ab}, \quad S_a = S_T = \mathcal{A} = \tilde{J}_a = 0. \tag{A15}$$

The result is

$$S^{(2)} = e^{-i\omega r_*} \frac{8\sqrt{4l+2}}{i\omega r} \frac{(l-1)(l+2)(r-1)}{[(l+2)(l-1)r+3]^2}, \tag{A16}$$

$$S^{(4)} = e^{-i\omega r_*} \frac{16\sqrt{(2l+3)\lambda_2}}{\sqrt{2\pi} i\omega r^3}$$
$$\times \frac{[(l^2+3l)(r^6-r^3)+5-4r^6-r^3]}{[(l+4)(l-1)r^3+10]^2}, \tag{A17}$$

$$S^{(6)} = e^{-i\omega r_*} \frac{6\sqrt{(2l+5)\lambda_4}}{\pi i\omega r^4}$$
$$\times \frac{[(l^2+5l)(r^{10}-r^5)+14-6r^{10}-8r^5]}{[(l+6)(l-1)r^5+21]^2}, \tag{A18}$$

$$S^{(8)} = e^{-i\omega r_*} \frac{4\sqrt{(2l+7)\lambda_6}}{\sqrt{3\pi^3} i\omega r^5}$$
$$\times \frac{[(l^2+7l)(r^{14}-r^7)+27-8r^{14}-19r^7]}{[(l+8)(l-1)r^7+36]^2}, \tag{A19}$$

where $\lambda_k \equiv [(l+k)(l+k-1)\dots(l+1)]$. The BH horizon r_h and the particle energy p_0 have been set equal to one. Equation (A16) coincides with Eq. (8) of Ref. [22].

APPENDIX B: ENERGY AND ANGULAR DISTRIBUTION

We derive here the formulas for the energy and the angular dependence of the gravitational emission. Gravitational waves in a $(n+2)$-dimensional spacetime behave asymptotically as $\sim r^{-n/2}$ [25] and possess $n(n+1)/2-1$ degrees of freedom. The transverse-traceless (TT) gauge is defined by $\delta g_{ab}=0$, $\delta g_{ai}=0$, and $\delta g_{ij}\gamma^{ij}=0$. These conditions can be chosen by imposing the harmonic gauge in the wave zone and using the remaining gauge freedom to constrain $\delta g_{tt}=0$, $\delta g_{ti}=0$, and $\gamma^{ij}\delta g_{ij}=0$.

We separate the angular part of the perturbations using tensor spherical harmonics, following Ref. [30]. In the TT gauge, the only nonvanishing term in the decomposition is the H_T component. Hence, the gauge invariant quantities for scalar perturbations (F and F_{ab}) depend only on H_T:

$$F = \frac{1}{n} H_T + \frac{1}{r}(D^a r)X_a, \quad F_{ab} = D_a X_b + D_b X_a, \tag{B1}$$

where

$$X_a = \frac{r^2}{\kappa^2} D_a H_T. \tag{B2}$$

The scalar perturbation Φ is written in terms of the gauge invariant quantities as

$$\Phi = \frac{n\tilde{Z} - r(X+Y)}{r^{n/2-1}[\kappa^2 - n + n(n+1)x/2]}, \tag{B3}$$

where

$$X+Y = -2nr^{n-2}F, \quad \tilde{Z} = \frac{1}{i\omega} r^{n-2} F^r{}_t. \tag{B4}$$

Setting

$$H_T \rightarrow \frac{A}{r^{n/2}} e^{i\omega r_*}, \tag{B5}$$

the asymptotic behavior of Φ is

$$\lim_{r\to\infty} \Phi = \frac{2A}{\kappa^2} e^{i\omega r_*}. \tag{B6}$$

The asymptotic behavior of h_{ij} in the TT gauge is

$$h_{ij}^{TT} = 2r^2 H_T \mathcal{S}_{ij} \sim \frac{\kappa^2 \Phi}{r^{n/2-2}} \mathcal{S}_{ij} = \frac{\Phi}{r^{n/2-2}} \left(D_i D_j \mathcal{S} + \frac{\kappa^2}{n} \gamma_{ij} \mathcal{S} \right). \tag{B7}$$

The energy-momentum pseudotensor does not depend on the spacetime dimension and is given by [25]

$$\frac{dE}{dSdt} = \langle t^{00} \rangle = \frac{\omega^2}{32\pi} \langle h_{ij}^{TT} h^{TTij} \rangle, \tag{B8}$$

where h_{ij}^{TT} are metric perturbations in the time domain. Using Parseval's theorem, the energy-momentum pseudotensor in the frequency domain is

$$\frac{dE}{dS d\omega} = \frac{\omega^2}{32\pi} \langle \tilde{h}_{ij}^{TT} \tilde{h}^{*TTij} \rangle, \tag{B9}$$

where $\tilde{h}_{ij}^{TT}$ are now the metric perturbations in the frequency domain. Substituting Eq. (B7) in Eq. (B9) we get

$$\frac{dE}{dS d\omega} = \frac{\omega^2}{32\pi} \frac{|\Phi|^2}{r^n} \left(D_i D_j \mathcal{S} + \frac{\kappa^2}{n} \gamma_{ij} \mathcal{S} \right)$$
$$\times \left(D_k D_l \mathcal{S}^* + \frac{\kappa^2}{n} \gamma_{kl} \mathcal{S}^* \right) \gamma^{ik} \gamma^{jl}. \tag{B10}$$

Integrating on the sphere $dS = r^n d\Omega_n$ and using the relations

$$D_i D^i \mathcal{S} = -\kappa^2 \mathcal{S}, \quad [D_j, D_i] V^j = R_{ki} V^k = (n-1) V_i, \tag{B11}$$

where V^i is a generic vector (here and in the following, indices are raised and lowered with γ^{ij}), we find the "two-sided" power spectrum

$$\frac{dE}{d\omega}^{two\text{-}sided} = \int dS^{(n)} \frac{dE}{dS d\omega} = \frac{\omega^2}{32\pi} \frac{n-1}{n} \kappa^2 (\kappa^2 - n) |\Phi|^2. \tag{B12}$$

The "one-sided" spectrum in Eq. (21) is obtained by multiplying Eq. (B12) by two. In the four-dimensional limit the one-sided spectrum is

$$\left. \frac{dE}{d\omega} \right|_{n=2} = \frac{\omega^2}{32\pi} \frac{(l+2)!}{(l-2)!} |\Phi|^2. \tag{B13}$$

Equation (B13) is Zerilli's formula for the lth multipole component of the energy spectrum in four dimensions. The total energy spectrum is given by the sum over the multipoles.

For each l the energy spectrum is

$$\frac{dE_l}{d\Omega d\omega} = \frac{\omega^2}{32\pi} |\Phi_l|^2 \left(D_i D_j \mathcal{S} + \frac{\kappa^2}{n} \gamma_{ij} \mathcal{S} \right)$$
$$\times \left(D^i D^j \mathcal{S}^* + \frac{\kappa^2}{n} \gamma^{ij} \mathcal{S}^* \right). \tag{B14}$$

Substituting Eq. (B12) in the previous equation, we find

$$\frac{dE_l}{d\Omega d\omega} = \frac{dE_l}{d\omega} \frac{n}{n-1} \frac{1}{\kappa^2 (\kappa^2 - n)} \left(D_i D_j \mathcal{S} + \frac{\kappa^2}{n} \gamma_{ij} \mathcal{S} \right)$$
$$\times \left(D^i D^j \mathcal{S}^* + \frac{\kappa^2}{n} \gamma^{ij} \mathcal{S}^* \right). \tag{B15}$$

The angular dependence for the lth multipole is obtained by integrating over frequency [22]. The result is

$$\frac{dE_l}{d\Omega} = \Delta E_l \frac{n}{n-1} \frac{1}{\kappa^2 (\kappa^2 - n)} \left(D_i D_j \mathcal{S} + \frac{\kappa^2}{n} \gamma_{ij} \mathcal{S} \right)$$
$$\times \left(D^i D^j \mathcal{S}^* + \frac{\kappa^2}{n} \gamma^{ij} \mathcal{S}^* \right) \equiv \Delta E_l \Lambda_l(\theta), \tag{B16}$$

where

$$\Lambda_l(\theta) = \frac{1}{\kappa^2 (\kappa^2 - n)} \left(\frac{n}{n-1} \mathcal{S}_{,\theta\theta} + \frac{k}{n-1} \mathcal{S} \right)^2. \tag{B17}$$

For $n = 2$ Eq. (B17) reduces to the known result in four dimensions [22]. The angular dependence is obtained by summing over the multipoles:

$$\frac{dE}{d\Omega}(\theta) = \sum_l \frac{dE_l}{d\Omega} = \sum_l \Delta E_l \Lambda_l(\theta). \tag{B18}$$

The result truncated to $l_{max} = 15$ is shown in the left panel of Fig. 4. The curve corresponding to $n = 2$ shows good agreement with Fig. 3 of Ref. [22].

[1] I. Antoniadis, Phys. Lett. B **246**, 377 (1990); N. Arkani-Hamed, S. Dimopoulos, and G.R. Dvali, *ibid.* **429**, 263 (1998); I. Antoniadis, N. Arkani-Hamed, S. Dimopoulos, and G.R. Dvali, *ibid.* **436**, 257 (1998); L. Randall and R. Sundrum, Phys. Rev. Lett. **83**, 3370 (1999); **83**, 4690 (1999).

[2] G.F. Giudice, R. Rattazzi, and J.D. Wells, Nucl. Phys. **B544**, 3 (1999); T. Han, J.D. Lykken, and R.J. Zhang, Phys. Rev. D **59**, 105006 (1999); J.L. Hewett, Phys. Rev. Lett. **82**, 4765 (1999); T.G. Rizzo, Phys. Rev. D **59**, 115010 (1999).

[3] T. Banks and W. Fischler, hep-th/9906038; S.B. Giddings and S. Thomas, Phys. Rev. D **65**, 056010 (2002); S. Dimopoulos and G. Landsberg, Phys. Rev. Lett. **87**, 161602 (2001); S. Dimopoulos and R. Emparan, Phys. Lett. B **526**, 393 (2002); R. Casadio and B. Harms, Int. J. Mod. Phys. A **17**, 4635 (2002); E.J. Ahn, M. Cavaglià, and A.V. Olinto, Phys. Lett. B **551**, 1 (2003).

[4] J.L. Feng and A.D. Shapere, Phys. Rev. Lett. **88**, 021303 (2002); A. Ringwald and H. Tu, Phys. Lett. B **525**, 135 (2002); E.J. Ahn, M. Ave, M. Cavaglià, and A.V. Olinto, Phys. Rev. D **68**, 043004 (2003).

[5] S. Hossenfelder, S. Hofmann, M. Bleicher, and H. Stocker, Phys. Rev. D **66**, 101502 (2002); K. Cheung, Phys. Rev. Lett. **88**, 221602 (2002); S.I. Dutta, M.H. Reno, and I. Sarcevic, Phys. Rev. D **66**, 033002 (2002); K. Cheung, *ibid.* **66**, 036007 (2002); E.J. Ahn and M. Cavaglià, Gen. Relativ. Gravit. **34**, 2037 (2002); V. Frolov and D. Stojkovic, Phys. Rev. D **66**, 084002 (2002); T. Han, G.D. Kribs, and B. McElrath, Phys. Rev. Lett. **90**, 031601 (2003); V. Frolov and D. Stojkovic, *ibid.* **89**, 151302 (2002); I. Mocioiu, Y. Nara, and I. Sarcevic, Phys. Lett. B **557**, 87 (2003); A. Chamblin, F. Cooper, and G.C. Nayak, Phys. Rev. D **69**, 065010 (2004).

[6] M. Cavaglià, Int. J. Mod. Phys. A **18**, 1843 (2003).

[7] K.S. Thorne, in *Magic without Magic: John Archibald Wheeler*, edited by J. Klauder (Freeman, San Francisco, 1972).

[8] M. Cavaglià, S. Das, and R. Maartens, Class. Quantum Grav. **20**, L205 (2003); S. Hossenfelder, M. Bleicher, S. Hofmann, H. Stocker, and A.V. Kotwal, Phys. Lett. B **566**, 233 (2003).

[9] M. Cavaglià, Phys. Lett. B **569**, 7 (2003).

[10] H. Yoshino and Y. Nambu, Phys. Rev. D **67**, 024009 (2003).

[11] O.I. Vasilenko, hep-th/0305067.

[12] P.D. D'Eath and P.N. Payne, Phys. Rev. D **46**, 658 (1992); **46**, 675 (1992); **46**, 694 (1992); D.M. Eardley and S.B. Giddings, *ibid.* **66**, 044011 (2002); H. Yoshino and Y. Nambu, *ibid.* **66**, 065004 (2002); D. Ida and K.I. Nakao, *ibid.* **66**, 064026 (2002).

[13] P.C. Aichelburg and R.U. Sexl, Gen. Relativ. Gravit. **2**, 303 (1971).

[14] http://lhc-new-homepage.web.cern.ch/lhc-new-homepage/

[15] R.J. Gleiser, C.O. Nicasio, R.H. Price, and J. Pullin, Phys. Rep. **325**, 41 (2000).

[16] P. Anninos and S. Brandt, Phys. Rev. Lett. **81**, 508 (1998).

[17] T. Regge and J.A. Wheeler, Phys. Rev. **108**, 1063 (1957).

[18] F. Zerilli, Phys. Rev. D **2**, 2141 (1970).

[19] M. Davis, R. Ruffini, W.H. Press, and R.H. Price, Phys. Rev. Lett. **27**, 1466 (1971).

[20] R. Ruffini, Phys. Rev. D **7**, 972 (1973); R. Ruffini and V. Ferrari, Phys. Lett. B **98**, 381 (1981); C. Lousto and R.H. Price, Phys. Rev. D **55**, 2124 (1997).

[21] J. Baker, B. Brugmann, M. Campanelli, C.O. Lousto, and R. Takahashi, Phys. Rev. Lett. **87**, 121103 (2001); Y. Mino, M. Sasaki, M. Shibata, H. Tagoshi, and T. Tanaka, Prog. Theor. Phys. Suppl. **128**, 1 (1997); S. Chandrasekhar, *The Mathematical Theory of Black Holes* (Oxford University Press, Oxford, 1983).

[22] V. Cardoso and J.P. Lemos, Phys. Lett. B **538**, 1 (2002).

[23] V. Cardoso and J.P. Lemos, Gen. Relativ. Gravit. **35**, 327 (2003).

[24] L. Smarr, Phys. Rev. D **15**, 2069 (1977).

[25] V. Cardoso, O.J. Dias, and J.P. Lemos, Phys. Rev. D **67**, 064026 (2003).

[26] V. Cardoso, S. Yoshida, O.J. Dias, and J.P. Lemos, Phys. Rev. D **68**, 061503 (2003).

[27] A.O. Barvinsky and S.N. Solodukhin, Nucl. Phys. **B675**, 159 (2003).

[28] S. Hollands and A. Ishibashi, gr-qc/0304054.

[29] H. Kodama, A. Ishibashi, and O. Seto, Phys. Rev. D **62**, 064022 (2000).

[30] H. Kodama and A. Ishibashi, Prog. Theor. Phys. **110**, 701 (2003).

[31] A. Ishibashi and H. Kodama, Prog. Theor. Phys. **110**, 901 (2003).

[32] H. Kodama and A. Ishibashi, Prog. Theor. Phys. **111**, 29 (2004).

[33] R.A. Konoplya, Phys. Rev. D **68**, 024018 (2003).

[34] R.A. Konoplya, Phys. Rev. D **68**, 124017 (2003).

[35] F.R. Tangherlini, Nuovo Cimento **27**, 636 (1963).

[36] G. Gibbons and S.A. Hartnoll, Phys. Rev. D **66**, 064024 (2002).

[37] I.P. Neupan, Phys. Rev. D (to be published), hep-th/0302132.

[38] K.D. Kokkotas and B.G. Schmidt, Living Rev. Relativ. **2**, 2 (1999); H.-P. Nollert, Class. Quantum Grav. **16**, R159 (1999).

[39] S. Iyer and C.M. Will, Phys. Rev. D **35**, 3621 (1987).

[40] S. Iyer, Phys. Rev. D **35**, 3632 (1987).

[41] S. Hod, Phys. Rev. Lett. **81**, 4293 (1998).

[42] L. Motl and A. Neitzke, Adv. Theor. Math. Phys. **7**, 307 (2003).

[43] D. Birmingham, Phys. Lett. B **569**, 199 (2003).

[44] O. Dreyer, Phys. Rev. Lett. **90**, 081301 (2003); G. Kunstatter, *ibid.* **90**, 161301 (2003); L. Motl, Adv. Theor. Math. Phys. **6**, 1135 (2003); E. Berti and K.D. Kokkotas, Phys. Rev. D **67**, 064020 (2003); V. Cardoso and J.P. Lemos, *ibid.* **67**, 084020 (2003); C. Molina, *ibid.* **68**, 064007 (2003); A. Neitzke, hep-th/0304080; A. Maassen van den Brink, Phys. Rev. D **68**, 047501 (2003); V. Cardoso, R. Konoplya, and J.P. Lemos, *ibid.* **68**, 044024 (2003); D. Birmingham, S. Carlip, and Y.J. Chen, Class. Quantum Grav. **20**, L239 (2003); E. Berti, V. Cardoso, K.D. Kokkotas, and H. Onozawa, Phys. Rev. D **68**, 124018 (2003); N. Andersson and C.J. Howls, Class. Quantum Grav. **21**, 1623 (2004); S. Hod, gr-qc/0307060; S. Yoshida and T. Futamase, Phys. Rev. D **69**, 064025 (2004); S. Musiri and G. Siopsis, Class. Quantum Grav. **20**, L285 (2003); J. Oppenheim, Phys. Rev. D **69**, 044012 (2004).

[45] S. Weinberg, *Gravitation and Cosmology* (Wiley, New York, 1972).

[46] V. Cardoso and J.P. Lemos, Phys. Rev. D **66**, 064006 (2002).

[47] M. Abramowitz and I. A. Stegun, *Handbook of Mathematical Functions* (Dover, New York, 1970); useful information can also be found at http://www.mathworld.wolfram.com.